

# Millimeter-wave dielectrics of indialite/cordierite glass ceramics: Estimating Si/Al ordering by volume and covalency of Si/Al octahedron

Hitoshi OHSATO,<sup>†</sup> Jeong-Seog KIM,\* Chae-II CHEON\* and Isao KAGOMIYA\*\*

Department of Research, Nagoya Industrial Science Research Institute, 2F Noa-Yotsuya Building,  
1-13 Yotsuya-dori, Chikusa-ku, Nagoya 464-0819, Japan

\*Department of Material Science and Engineering, Hoseo University,  
165 Sechul-ri, Baebang-myeon, Asan-si Chungnam 336-795, Korea

\*\*Material Science and Engineering, Nagoya Institute of Technology, Gokiso-cho, Showa-ku, Nagoya 466-8555, Japan

Cordierite ( $\text{Mg}_2\text{Al}_4\text{Si}_5\text{O}_{18}$ ) is a candidate for millimeter-wave dielectrics, and has two polymorphs due to ordering of Si and Al ions on  $\text{Si}/\text{AlO}_4$  tetrahedra: disordered high symmetry form called as indialite and ordered low symmetry form cordierite. Indialite/cordierite glass ceramics exhibited much higher  $Qf$  value of 200,000 GHz than conventional solid state reaction ceramics of 40,000 GHz, which were fabricated by crystallization of glass pellet. The glass ceramics having indialite as a dominant phase showed high  $Qf$ . The crystal phases are analyzed by Rietveld method. In this paper, the ordering ratios of indialite and cordierite are estimated by the volumes and covalencies of  $\text{Si}/\text{AlO}_4$  tetrahedra.

©2013 The Ceramic Society of Japan. All rights reserved.

Key-words : Millimeter-wave dielectrics, Indialite/cordierite, Glass ceramics, Superior high Q, Low dielectric constant, Ordering

[Received April 16, 2013; Accepted June 23, 2013]

## 1. Introduction

Millimeter-wave wireless communications with high data transfer rate for non-compressed digital video transmission system and radar for Pre-Crash Safety System have been developed recently. These systems for millimeter-wave wireless communications require dielectric substrates with high quality factor ( $Qf$ ), low dielectric constant ( $\epsilon_r$ ), and near zero temperature coefficient of resonance frequency ( $TCf$ ).<sup>1)</sup> They also require other physical properties such as high thermal conductivity and low thermal expansion.<sup>2)</sup> Millimeter-wave dielectrics are required to have high  $Qf$  because the utilizations at high frequency causes high dielectric losses, and also low dielectric constants for accuracy control of the fabrication. Since the substrates in a radar system are exposed to a wide range of temperature inside a narrow space between the front of the engine room and the radiator, the  $TCf$  of the substrates should be tuned to near-zero. Ceramics substrates are more superior than resin substrates, because of their high  $Qf$ , near-zero  $TCf$ , high thermal conductivity, and low thermal expansion. Silicates are suitable for millimeter-wave dielectrics because of their low dielectric constant, and the crystal structure consists of silicon tetrahedron  $\text{SiO}_4$  with 50% covalency.<sup>1)</sup> Cordierite ( $\text{Mg}_2\text{Al}_4\text{Si}_5\text{O}_{18}$ ) is one of the silicates that have good dielectric properties, which has high  $Qf$  of 40,000 GHz,  $\epsilon_r$  of 6.2, and  $TCf$  of  $-24 \text{ ppm}/^\circ\text{C}$ .<sup>3)</sup> This  $TCf$  value is better than that of other substrates having low dielectric constant of ca.  $-60 \text{ ppm}/^\circ\text{C}$ .

Cordierite has two polymorphs: cordierite and indialite as shown in Figs. 1(a) and 1(c), respectively. Cordierite is of low symmetry form: orthorhombic crystal system  $Cccm$  (No. 66),

which has  $\text{Si}_4\text{Al}_2\text{O}_{18}$  six-membered tetrahedron rings with ordered  $\text{SiO}_4$  and  $\text{AlO}_4$  tetrahedra as shown in Fig. 1(b). On the other hand, indialite is of high symmetry form: hexagonal crystal system  $P6/mcc$  (No. 192), which has disordered  $\text{Si}_4\text{Al}_2\text{O}_{18}$  equilateral hexagonal rings.<sup>4)</sup>

As presented in the previous papers,<sup>3)</sup> the  $Qf$  values of Ni-doped cordierite ( $\text{Mg}_{2-x}\text{Ni}_x\text{Al}_4\text{Si}_5\text{O}_{18}$ ) ceramics were improved from 40,000 to 90,000 GHz.<sup>3)</sup> The volumes and covalencies of the  $\text{Si}/\text{AlO}_4$  tetrahedra in the Ni-doped samples remain at similar level of values regardless of increasing Ni concentration ( $x$ ) as shown in Figs. 2(b) and 2(c), respectively. These phenomena reveal the disordering of Si and Al on the  $\text{Si}/\text{AlO}_4$  tetrahedra, which tend to change its crystal structure from cordierite to indialite. The volumes and covalencies were calculated by the atomic coordinates of Ni-doped cordierite, obtained by X-ray crystal structure by Rietveld method.

In this paper, previous results of indialite/cordierite glass ceramics with superior high  $Q$  value<sup>5)</sup> are reviewed, and Si/Al orderings are estimated based on the calculated volumes and the covalencies of  $\text{Si}/\text{AlO}_4$  tetrahedra.

## 2. Experimental procedure

Powder materials with cordierite/indialite  $\text{Mg}_2\text{Al}_4\text{Si}_5\text{O}_{18}$  composition were prepared by using high purity raw materials:  $\text{MgO}$ ,  $\text{Al}_2\text{O}_3$  and  $\text{SiO}_2$  ( $>99.9 \text{ wt}\%$  purity). The powders were ball-milled and calcined for decarboxylation, and were melted at  $1550^\circ\text{C}$  and refined for removing small air seeds at  $1600^\circ\text{C}$  in Pt-crucible with 40 cc, and casted in graphite mold of  $\phi 10 \times 30 \text{ mm}$ . The glass rods were annealed for relieving the thermal stress at  $760^\circ\text{C}$  for 1 h under the glass transition temperature ( $T_g$ ) of  $780^\circ\text{C}$ . The  $T_g$  was obtained by differential thermal analysis (DTA) as described later. Glass pellets with  $\phi 10 \times 6 \text{ mm}$  were cut and crystallized at 1200 to  $1440^\circ\text{C}$  for 10 and

<sup>†</sup> Corresponding author: H. Ohsato; E-mail: ohsato.hitoshi@nitech.ac.jp

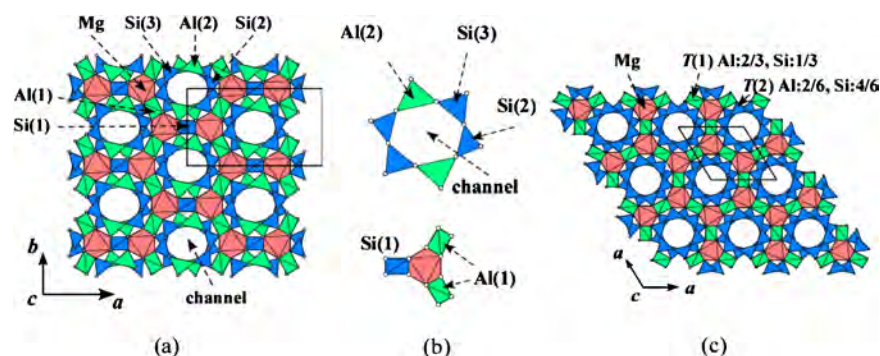


Fig. 1. Crystal structure of the low symmetry form of cordierite with orthorhombic system *Cccm* (No. 66) (a), Si/Al<sub>2</sub>O<sub>4</sub> ordered tetrahedra located in hexagonal rings and among the rings (b), and high symmetry form indialite with hexagonal system, *P6/mcc* (No. 192) (c).

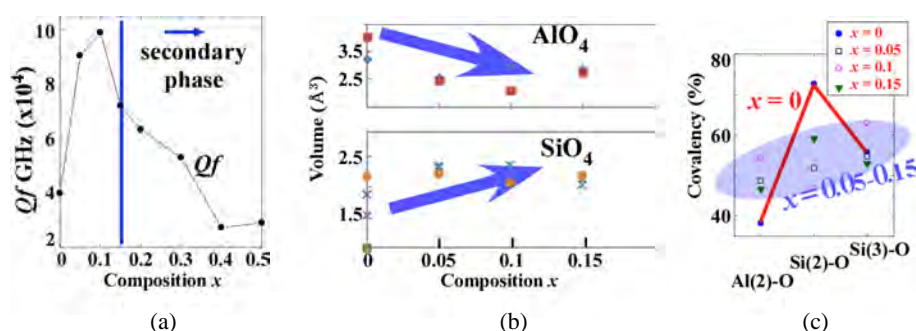


Fig. 2. Millimeter-wave dielectric properties  $Qf$  of Ni-doped  $(\text{Mg}_{1-x}\text{Ni}_x)_2\text{Al}_4\text{Si}_5\text{O}_{18}$  ( $x = 0-0.5$ ) ceramics  $Qf$  (a). Volumes (b) of  $\text{SiO}_4$  and  $\text{AlO}_4$ , and covalencies (c) of Si and Al as a function of composition  $x$ .

20 h. The crystallized samples were polished to the thickness up to a half of the diameter, and took optical microscope photos, scanning electron microscope (SEM) image (FEI, Quanta 200 FEG), X-ray powder diffraction (XRPD, Rigaku, Rad-C model), and millimeter-wave dielectrics  $\epsilon_r$ ,  $Qf$  and  $TCf$  by Hakki and Coleman method.<sup>6),7)</sup> The crystal structural analysis for the coordinates, the bond lengths and the crystalline phase ratios between indialite and cordierite was performed by Rietveld method (Fullprof software<sup>8)</sup>) using XRPD data which was taken by step scanning  $0.02^\circ$  for 10 s/step by monochromatized  $\text{CuK}\alpha$  radiation generated by an X-ray tube 40 KV 20 mA. The original coordinates of indialite and cordierite were obtained from the ICSD (36248<sup>9)</sup>) and ICSD (30947<sup>10)</sup> & 86344<sup>11)</sup>), respectively, and the site occupancies are adopted ideal ones.

Si/Al ordering ratio could not be obtained directly from the structural analysis due to similar atomic scattering factors of Si and Al. The Si/Al ordering was estimated from the calculated volumes and covalencies of Si/Al<sub>2</sub>O<sub>4</sub> tetrahedra derived from the atomic coordinates obtained by Rietveld method. Covalencies of Si/Al<sub>2</sub>O<sub>4</sub> tetrahedra were calculated based on the bond length by Broun et al.<sup>12),13)</sup>

### 3. Results and discussion

#### 3.1 Preparation of glass ceramics

The glass rods shown in Fig. 3(a) having high strain [Fig. 3(b)] are stress-relieved as shown in Fig. 3(c) by the annealing at  $760^\circ\text{C}$  that is slightly below the  $T_g$ . The  $T_g$  was determined from the DTA curve as shown in Fig. 4. Here, P1 and P2 peaks in DTA curve may be crystallization temperature of  $\beta$ -quartz solid solutions<sup>14)</sup> (another name:  $\mu$ -cordierite), and indialite, respective-

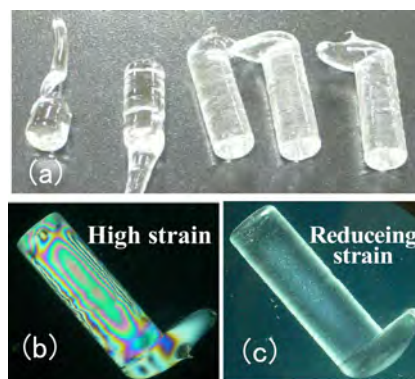


Fig. 3. (a) Casting glass rods (10  $\phi$   $\times$  30 mm). As-casted glass with high strain (b) and reducing strain by annealing (c) under the crossed polars.

ly,<sup>15),16)</sup> and P3 and P4 peaks are not clear. Figure 5(a) shows the XRPD patterns from the surface of glass pellets crystallized at various temperatures. The  $2\theta$  positions of the diffraction lines remained unchanged, and the intensities of diffraction peaks randomly changed on all XRPD patterns. Figure 5(b) shows XRPD patterns of the same samples [Fig. 5(a)] after pulverizing into powder form, which patterns are identified as indialite/cordierite. They show anisotropic crystal growth from glass surface as shown in Fig. 6. This anisotropic growth brings in cracks as shown in Fig. 7(a), because the thermal expansions of  $a$ - and  $c$ -axis are opposite signs as shown in Fig. 8.<sup>17),18)</sup> Moreover,

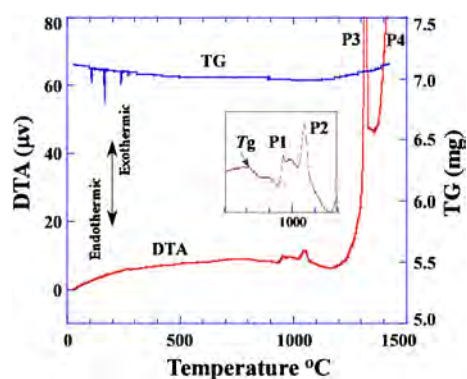


Fig. 4. DTA curves of cordierite glass with magnified figure around glass transition  $T_g$ .

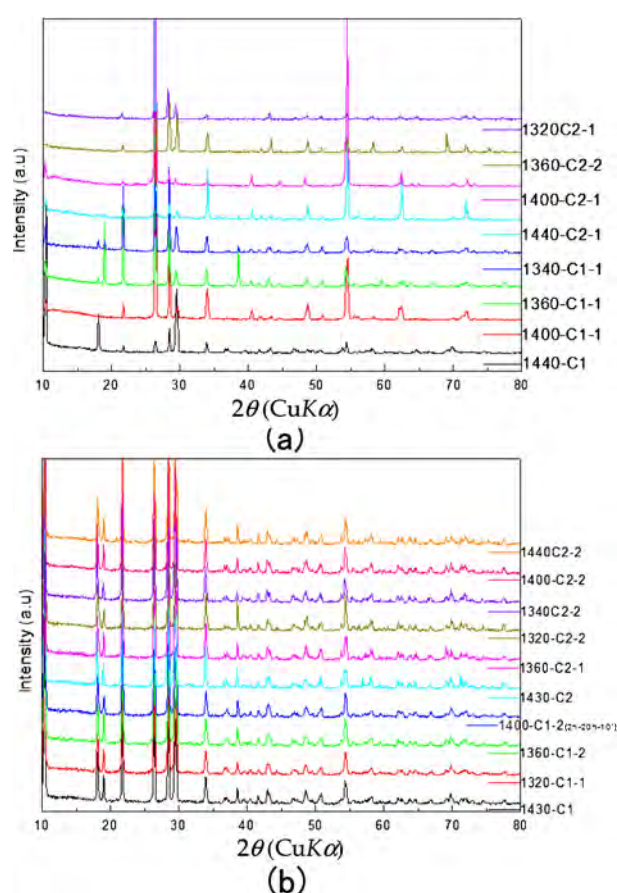


Fig. 5. (a) XRPD patterns from pellet surface showing anisotropic crystal growth. (b) XRPD patterns by powdered samples showing ordinary peak intensity.

deformation was occurred as shown in Fig. 7(b), which deformation originated from the formation of glass phase as shown in Fig. 7(c). The cracks could be avoided by slow cooling after sintering. And the deformations could be avoided by reducing the formation the glass phase by means of rapidly heating to the peak temperature P3 shown in Fig. 4.

### 3.2 Millimeter-wave dielectric properties

Figures 9(a)–9(c) show the amount of indialite (a) and millimeter-wave dielectric properties of the samples sintered at 1200 to 1440°C for 10 and 20 h [(b) and (c)], respectively. The amounts of indialite are 94.6 and 91.5% in the samples sintered at ca. 1200°C for 10 and 20 h, respectively. And the indialite decrease to 18.5 and 13.7% at ca. 1400°C for 10 and 20 h, respectively. The amounts of indialite and cordierite are obtained by Rietveld analysis.<sup>8)</sup> The analyzed data are presented in Table 1, which data is a re-analysed one based on the previous data.<sup>5)</sup> Interestingly the amount of indialite decreases with the sintering temperature. Based on these results, we could temporarily conclude that the indialite phase with high symmetry is an intermediate phase. Generally crystals undergo a phase transition

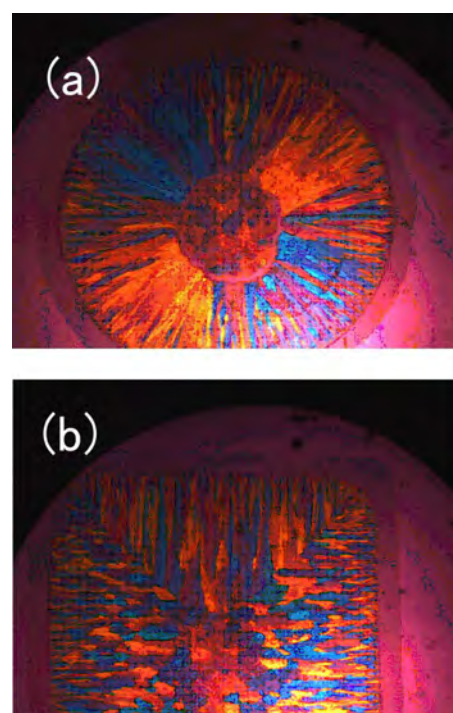


Fig. 6. Anisotropic crystal growth from crystal surface under crossed polars. (a) perpendicular to glass rod, (b) parallel to glass rod.

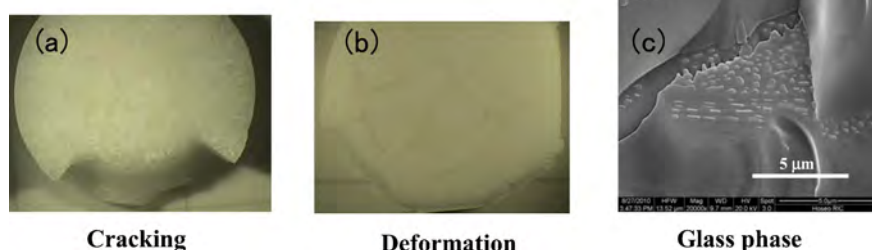


Fig. 7. (a) Cracking of pellet by anisotropic crystal growth. (b) Deformation of pellet by formation of glass as shown in (c).



to a high symmetry from a low symmetry as increasing temperature. However, in the samples, with increasing the crystallization temperature the phase transits to a low symmetry from a high symmetry phase.<sup>19)</sup>

The quality factors  $Qf$  ( $\sim 200,000$  GHz) of these indialite/cordierite glass ceramics are superior compared to that of cordierite ceramics ( $\sim 40,000$  GHz) synthesized by solid state reaction as shown in Fig. 9(c), which figures are suitable level for millimeter-wave dielectrics. However, the measured  $Qf$  values in these samples showed a wide scattering range, which are dependent on the sintering conditions in each sample. Most of the samples show cracks and deformation as shown in Figs. 7(a) and 7(b), respectively. The  $Qf$  values decrease as a function of crystallization temperature as shown in Figs. 9(b) and 9(c). From the relationship between the  $Qf$  and the phase proportions as shown in Fig. 9(a), we can conclude the indialite glass ceramics exhibit high quality factor than the cordierite ones. The dielectric constants and  $TCf$  values of all samples [see Figs. 9(b) and 9(c)] are about 4.6, and  $-26$  ppm/ $^{\circ}\text{C}$ , respectively.

### 3.3 Estimation of Si/Al ordering

The atomic coordinates of indialite and cordierite phases in the glass ceramics crystallized at 1200, 1300 and 1400 $^{\circ}\text{C}$  for 10 h are shown in Tables 2(a) and 2(b), respectively. They are by using indialite and cordierite mixed models by Rietveld method.<sup>8)</sup>

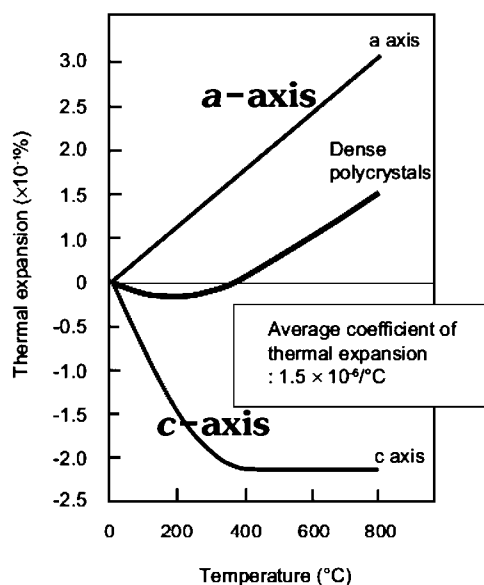
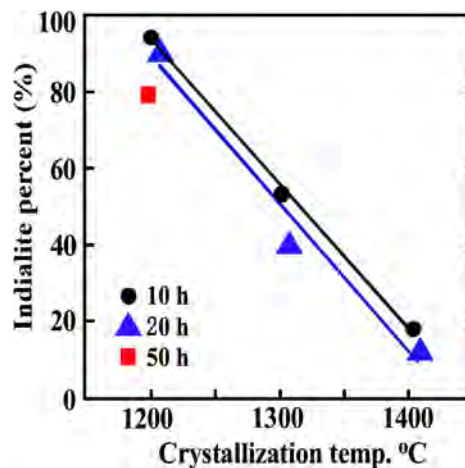


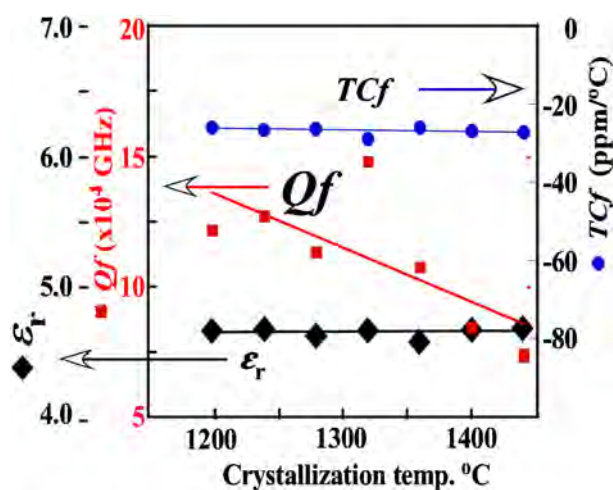
Fig. 8. Anisotropic thermal expansion of cordierite.<sup>14)</sup>

Table 1. Amount of indialite and cordierite in glass ceramics revised<sup>5)</sup>

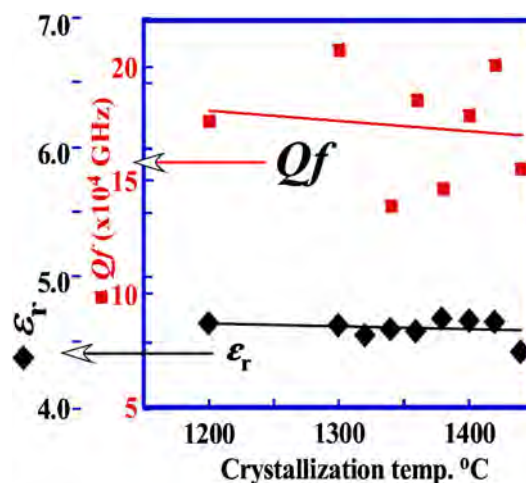
| Crystallization temperature<br>( $^{\circ}\text{C}$ -h) | Indialite<br>(%) | Cordierite<br>(%) |
|---|------------------|-------------------|
| 1200-10   | 94.64            | 5.36              |
| 1300-10   | 53.62            | 46.38             |
| 1400-10   | 18.52            | 81.48             |
| 1200-50   | 78.63            | 21.37             |
| 1210-20   | 91.52            | 8.48              |
| 1310-20   | 40.83            | 59.17             |
| 1410-20   | 13.66            | 86.34             |
| 1210-30   | 53.69            | 46.31             |
| 1210-40   | 48.64            | 51.36             |
| 1210-50   | 41.07            | 58.93             |



(a)



(b)



(c)

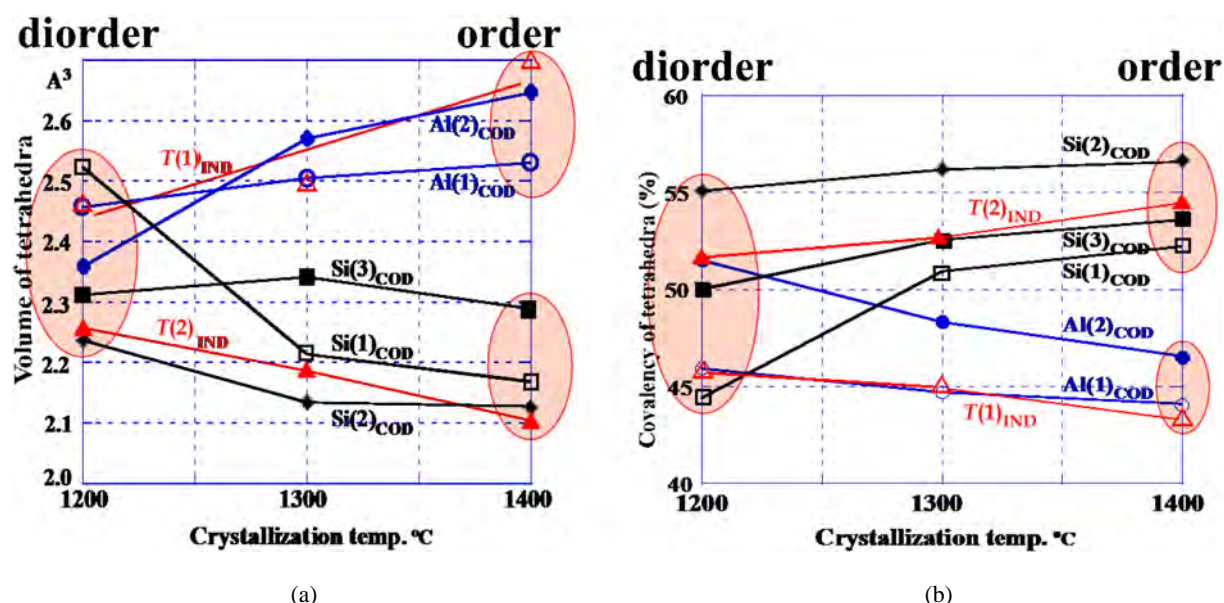
Fig. 9. (a) Amount of indialite, and (b) and (c) millimeter-wave dielectric properties of crystallized at 1200–1400 $^{\circ}\text{C}$  for 10 and 20 h, respectively.

Table 2(a). Coordinates of indialite crystallized at 1200, 1300 and 1400°C for 10 h

| Name | Multiplicity<br>Wyckoff letter | 1200°C 10 h |           |           | 1300°C 10 h |           |          | 1400°C 10 h |          |          |
|------|--------------------------------|-------------|-----------|-----------|-------------|-----------|----------|-------------|----------|----------|
|      |                                | x           | y         | z         | x           | y         | z        | x           | y        | z        |
| Mg   | 4c                             | 1/3         | 2/3       | 1/4       | 1/3         | 2/3       | 1/4      | 1/3         | 2/3      | 1/4      |
| T(1) | 6f                             | 1/2         | 1/2       | 1/4       | 1/2         | 1/2       | 1/4      | 1/2         | 1/2      | 1/4      |
| T(2) | 12l                            | 0.3729(2)   | 0.2664(2) | 0         | 0.3758(6)   | 0.2678(7) | 0        | 0.357(2)    | 0.261(2) | 0        |
| O(1) | 24m                            | 0.4859(3)   | 0.3489(3) | 0.1441(3) | 0.4861(9)   | 0.3508(7) | 0.139(1) | 0.478(2)    | 0.346(2) | 0.134(2) |
| O(2) | 12l                            | 0.2328(4)   | 0.3107(3) | 0         | 0.239(1)    | 0.318(1)  | 0        | 0.219(3)    | 0.295(3) | 0        |

Table 2(b). Coordinates of cordierite crystallized at 1200, 1300 and 1400°C for 10 h

| Name  | Position<br>Multiplicity<br>Wyckoff letter | 1200°C 10 h |           |          | 1300°C 10 h |            |           | 1400°C 10 h |            |           |
|-------|--|-------------|-----------|----------|-------------|------------|-----------|-------------|------------|-----------|
|       |  | x           | y         | z        | x           | y          | z         | x           | y          | z         |
| Mg    | 8g   | 0.338(2)    | 0         | 1/4      | 0.3363(4)   | 0          | 1/4       | 0.3373(2)   | 0          | 1/4       |
| Al(1) | 8k   | 1/4         | 1/4       | 0.273(3) | 1/4         | 1/4        | 0.2542(9) | 1/4         | 1/4        | 0.2534(5) |
| Al(2) | 8l   | 0.047(1)    | 0.312(4)  | 0        | 0.0476(4)   | 0.3038(7)  | 0         | 0.0512(2)   | 0.3093(4)  | 0         |
| Si(1) | 4b   | 0           | 1/2       | 1/4      | 0           | 1/2        | 1/4       | 0           | 1/2        | 1/4       |
| Si(2) | 8l   | 0.181(2)    | 0.069(3)  | 0        | 0.1894(4)   | 0.0758(7)  | 0         | 0.1920(2)   | 0.0774(4)  | 0         |
| Si(3) | 8l   | 0.121(2)    | -0.231(3) | 0        | 0.1355(4)   | -0.2375(7) | 0         | 0.1352(2)   | -0.2392(4) | 0         |
| O(1)  | 8l   | 0.030(3)    | -0.239(7) | 0        | 0.0431(7)   | -0.248(1)  | 0         | 0.0429(4)   | -0.2526(8) | 0         |
| O(2)  | 8l   | 0.089(3)    | 0.157(6)  | 0        | 0.1175(7)   | 0.181(1)   | 0         | 0.1220(4)   | 0.1876(7)  | 0         |
| O(3)  | 8l   | 0.141(3)    | -0.054(6) | 0        | 0.1596(8)   | -0.078(1)  | 0         | 0.1631(4)   | -0.0807(7) | 0         |
| O(4)  | 16m  | 0.236(2)    | -0.089(4) | 0.346(4) | 0.2440(6)   | -0.1012(8) | 0.353(1)  | 0.2461(3)   | -0.1002(5) | 0.3566(6) |
| O(5)  | 16m  | -0.066(3)   | 0.422(4)  | 0.358(6) | -0.0648(5)  | 0.4179(8)  | 0.350(1)  | -0.0637(3)  | 0.4168(5)  | 0.3493(7) |
| O(6)  | 16m  | -0.176(2)   | -0.307(4) | 0.357(4) | -0.1734(5)  | -0.3146(8) | 0.352(1)  | -0.1743(3)  | -0.3140(5) | 0.3553(6) |

Fig. 10. Estimating the ordering ratios of Si and Al in tetrahedra by volumes (a) and covalencies (b) of Si/AlO<sub>4</sub> tetrahedra.

The weighted reliability factors  $R_{wp}$ s for these samples are 2.94, 3.02 and 2.96% for indialite, 5.74, 3.69 and 3.32% for cordierite, which were crystallized at 1200, 1300 and 1400°C, respectively.

We can infer the ordering ratio of Si and Al on the tetrahedra from the volumes and covalencies on Si/AlO<sub>4</sub> tetrahedra. The volumes and covalencies of Si/AlO<sub>4</sub> tetrahedra for indialite and cordierite phases formed at 1200, 1300 and 1400°C were calculated from the coordinates obtained by Rietveld analysis, and they are shown in Figs. 10(a) and 10(b), respectively. There are two sites of tetrahedra in indialite: one is T(1) located among the

rings, another is T(2) in the hexagonal ring as shown in Fig. 1(c). And there are five sites of tetrahedra in cordierite: Al(1) and Si(1) locate among the hexagonal rings, and Al(2), Si(2), and Si(3) locate inside the ring as shown in Fig. 1(b). All the volumes of the tetrahedra at 1200°C converged to a range of 2.2–2.5 Å<sup>3</sup> as shown in Fig. 10(a), which indicates disordering of Si and Al ions. And T(1), Al(1) and Al(2) increase to around 2.6 Å<sup>3</sup> at 1400°C. On the other hand, T(2), Si(1), Si(2) and Si(3) decrease to around 2.2 Å<sup>3</sup>. Here, ionic radii of Al<sup>3+</sup> and Si<sup>4+</sup> with coordination number (CN) 4 are 0.39 and 0.26, respectively. So,

the changes in the tetrahedral volumes depend on the ratio Al and Si in these sites. In the case of covalencies,  $T(2)$ , Si(1), Si(2) and Si(3) increase, and  $T(1)$ , Al(1) and Al(2) decrease as a function of crystallization temperature. Usually covalency of the  $\text{SiO}_4$  is larger than that of the  $\text{AlO}_4$  tetrahedron. Hence, in our results, the increase of covalencies of  $T(2)$ , Si(1), Si(2) and Si(3) sites at  $1400^\circ\text{C}$  should indicate that Si ions dominantly occupy these sites. On the other hand, the decrease of the covalencies of  $T(1)$ , Al(1) and Al(2) should indicate that Al ions occupy these sites.

#### 4. Conclusions

Previous works on indialite/cordierite glass ceramics was reviewed, and a new method for estimating Al/Si ordering was presented as follows:

- (1) Fabrication method of indialite/cordierites glass ceramics was presented.
- (2) The glass ceramics showed superior  $Qf$  of more than 200,000 GHz, low dielectric constant of 4.7, and low  $TCf$  of  $-26\text{ ppm}/^\circ\text{C}$ .
- (3) Indialite with high symmetry and high  $Qf$  formed at lower temperature than cordierite with low symmetry does.
- (4) The atomic coordinates of indialite and cordierite were obtained by Rietveld crystal structure analysis. Based on the coordinates obtained, the volumes and the covalencies of Si/ $\text{AlO}_4$  tetrahedra were calculated.
- (5) Ordering conditions were estimated by using the volumes and covalencies of the tetrahedra.

**Acknowledgements** The authors thanks to Dr. Chunting Lee for the measurement of millimeter-wave dielectric properties and Professor Ken'ichi Kakimoto for supporting research. A part of this study was supported by Grant-in Aid for Scientific Research (C), and Adaptable & Seamless Technology Transfer Program from the Ministry of Education, Culture, Sports, Science and Technology, Japan.

#### References

- 1) H. Ohsato, *Mater. Res. Soc. Symp. Proc.*, **833**, 55–62 (2005).
- 2) Fine Ceramics Center (JFCC): Report of support industrial project 2011, “R&D for ceramics substrates with low thermal expansion and high thermal conductivity”.
- 3) H. Ohsato, I. Kagomiya, M. Terada and K. Kakimoto, *J. Eur. Ceram. Soc.*, **30**, 315–318 (2010).
- 4) G. V. Gibbs, *Am. Mineral.*, **51**, 1068–1087 (1966).
- 5) H. Ohsato, J.-S. Kim, A.-Y. Kim, C.-I. Cheon and K.-W. Chae, *Jpn. J. Appl. Phys.*, **50** 09NF01 (2011).
- 6) B. W. Hakki and P. D. Coleman, *IRE Trans. Microwave Theor. Tech.*, **8**, 402–410 (1960).
- 7) Y. Kobayashi and M. Kato, *IEEE Trans. Microw. Theory Tech.*, **33**, 586–592 (1985).
- 8) Fullprof software by Juan Rodriguez-Carvajal in France, <http://www-llb.cea.fr/fullweb/powder.htm>.
- 9) A. Bystroem, *Arkiv foer Kemi, Mineralogi och Geologi*, **B**, **15**, 1–7 (1942).
- 10) T. Armbruster, *Neues Jahrb. Miner. Monatsh.*, **1985**, 255–267 (1985).
- 11) B. Winkler, M. T. Dove and M. Leslie, *Am. Mineral.*, **76**, 313–331 (1991).
- 12) I. D. Brown and R. D. Shannon, *Acta Crystallogr., Sect. A: Cryst. Phys., Diffir., Theor. Gen. Crystallogr.*, **29**, 266–282 (1973).
- 13) D. Brown and K.-K. Wu, *Acta Crystallogr., Sect. B: Struct. Crystallogr. Cryst. Chem.*, **32**, 1957–1959 (1976).
- 14) W. Schreger and J. F. Schairer, *Zeit. Krist.*, **116**, 60–82 (1961).
- 15) I. Uei, K. Inoue and M. Fukui, *Yogyo-Kyokai-Shi*, **74**, 325–335 (1966).
- 16) T. Sugimura, H. Ohsato and Y. Nakai, *Yogyo-Kyokai-Shi*, **82**, 48–54 (1974).
- 17) H. Ikawa, T. Otagiri, O. Imai, K. Urabe and S. Udagawa, *Yogyo-Kyokai-Shi*, **94**, 344–350 (1986).
- 18) I. Ogata, K. Mizutani, K. Makino and Y. Kobayashi, *DENSO Technical Review*, **13**, 112–118 (2008).
- 19) “Encyclopedia of fine ceramics”, ISEN: 4-7655-0016-0, Gihodo Shuppan Co., Ltd. (1987) pp. 179.